Ultra Wideband Dual Polarization Metamaterial Absorber for 5G frequency spectrum

Majid Amiri*, Farzad Tofigh, Negin Shariati, Justin Lipman, Mehran Abolhasan
*Dept. Electrical and Data Engineering , University of Technology Sydney, Sydney, Australia
Majid.Amiri@student.uts.edu.au*

***Abstract*—Implementing 5G technology contributes to improve communication quality and facilitate several interesting applications in daily life such as Internet of things. Despite outstanding features of 5G, the amount of ambient electromagnetic waves will be increased significantly in the environment, which may be undesired. Ultra-wideband metamaterial perfect absorber is a promising solution to collect these undesired signals. Using lumped elements in absorber structure to increase the absorption bandwidth leads to design and fabrication process complexity. In this paper, a low profile polarization angle selective metamaterial absorber has been designed to absorb signals in the frequency range of 21.79 GHz to 53.23 GHz with more than 90$\%$ efficiency. The relative absorption bandwidth of the final structure is 83.81$\%$. Moreover, the final structure is reasonably insensitive facing different incident angle up to 40 degree.**

***Index Terms*—5G, internet of things, metamaterial, absorber, ultra wideband, dual polarization.**

I. Introduction

Internet of things (IoT) is a fast growing technology, which targets lots of current applications to connect them to the internet. Autonomous devices with remote controlling capability, smart houses and cities are some of the interesting features of IoT technology. Considering the huge number of required electric devices and sensors, the reliable, low latency and wideband internet connection is crucial to implement this concept in the real world. 5G is a promising answer for most of the requisites in IoT regarding the connection challenges.

Besides all interesting features of IoT, increasing the usage of wireless communication provides the opportunity of reusing the electromagnetic signals energy. Meanwhile, collecting ambient electromagnetic energy leads to reducing the level of energy in some specific environment that ambient signals are an undesired parameter. Due to varieties of signal frequencies in 5G applications, absorbing signals from the environment needs a wideband receiver. Moreover, a high-efficiency structure is reacquired due to the low power level of ambient signals.

Metamaterial perfect absorber (MPA) has been introduced by Landy in 2008 to be used instead of bulky and costly conventional absorbers such as Ferrit and resistive sheets. However, due to the outstanding capabilities of MPA to absorb electromagnetic signals with near 100% efficiency, their usage have been expanded in various applications such as absorption of undesired frequency [1], [2], THz applications [3], [4], thermal emitters [5], [6], optical switches[7], [8] and energy harvesting [9], [10], [11]. Different characteristics are needed in each application based on targeted requisites.

Having an ultra-wide absorption band is one the crucial property which is required in most of the mentioned applications, especially eradication of undesired signals and energy harvesting. Different methods have been investigated to increase the absorption bandwidth. For instance, various sizes of resonators in co-planar structure have been used in several reports[12], [13], [14], [15], [16]. Moreover, the resonators have been located in a multi-layer structure. Compared to the co-planar structure, this topology leads to less mutual coupling and gives the freedom of using resonators with close size. This phenomenon causes merging absorption bands to provide a wideband metamaterial absorber [17], [18], [19]. However, these two methods increase the size and complexity of structure, respectively.

Using lumped elements is another method to design wideband metamaterial absorber. Additional to the lossy substrate, lumped resistors improve the structure absorptivity by increasing the dielectric resistance [20], [21], [22]. In wideband applications, the resistors improve bandwidth by enhancing the absorption ratio between resonance frequencies. Also, lumped capacitors and inductors are able to adjust the absorption frequencies [23]. Similar to previous methods, adding lumped elements increases the fabrication process.

In this paper, an ultra-wide absorption band metamaterial perfect absorber (MPA) using a simple structure has been proposed. The L-shape resonator with two parasitic L-shape elements has provided more than 21 GHz of bandwidth, which covers 5G frequency spectrum with more than90 $\%$ absorption efficiency. 5G technology will be implemented in various frequency ranges. Due to the limited bandwidth in commercial radio frequency (from 600 MHz to 7.1 GHz), 5G applications shift to the higher frequency spectrum, such as millimeter waves. These ranges vary in different countries. For instance, 27.5-28.35 GHz and 37-40 GHz in USA, and 24.25-27.5 GHz in Europe, and 27.5-28.25 GHzin Japan, and 24.25-27.5 GHz and 37.25-43.5 GHz in China, are some the 5G frequency spectrum in different countries.

Furthermore, the structure is reasonably low-cost and small due to using FR-4 substrate and nested resonators, respectively. Unlike the majority of wideband structures, the lumped elements have not been used, which simplifies the fabrication process. The structure has been investigated under different

incident angles for both TE and TM polarized waves. Results show absorption stability up to $\theta = 40$. The final structure has been analyzed using full-wave simulations in CST Studio under normal incident waves.

II. Unit Cell Design Principles

The basic principle of designing metamaterial absorber is perfect impedance matching with air intrinsic impedance. The absorption ratio of MPA is related to transmission and reflection coefficients. Ideally, the amount of return waves from surface would be near zero ($\Gamma(\omega) \approx 0$) in well-matched structure. Moreover, using metal film on the bottom of structure guarantees the zero wave transmission ($T(\omega) = 0$). It is noteworthy that the transmission and reflection coefficients are extracted from S parameters, where $T(\omega) = |S_{12}|^2$ and $\Gamma(\omega) = |S_{11}|^2$. Eventually, the absorption ratio is computed as below:

$$A(\omega) = 1 - \Gamma(\omega) - T(\omega) = 1 - |S_{11}|^2 - |S_{12}|^2 = 1 - |S_{11}|^2$$

The number of absorption bands is directly related to the number of resonators using in the structure. In this regard, the absorption bands could be merged to create a wideband absorber, if proper dimensions and positions have been chosen for resonators. The unit cell of the proposed metamaterial absorber in this paper includes 3 L-shape metal paths with different sizes and widths (shown in Fig. 1 (a)). The FR-4 is used as a substrate with $\varepsilon_r = 4.4$ ad $tan\delta = 0.02$ to provide a lossy environment to eradicate the trapped signal. The copper layers with thickness of 0.035mm and electric conductivity $\sigma = 5.96 \times 10^7 S/m$ are used. The thickness of the substrate is an essential factor in the absorption mechanism based on the transmission line modeling for metamaterial perfect absorber [24]. Due to this method, each resonator is considered as a series RLC circuit. Moreover, substrate dielectric combining with a metal film on the bottom of the structure modeled as a shorted transmission line with relative impedance of dielectric. In this paper, the thickness of FR-4 is $h = 1mm$. Fig. 1 (b) illustrates the equivalent circuit for designed absorber, which Z_0, Z_r, and Z_t represent air intrinsic, resonators, and transmission line impedance, respectively. The equivalent circuit clarifies the mechanism of MPA, and also different parts of structure individually. Having a clear map between MPA structure and equivalent lumped elements leads to more applicable manipulation aiming to desired MPA characteristics.

Considering the equivalent circuit, the absorption ratio can be also defined as below:

$$A(\omega) = 1 - \Gamma(\omega) = 1 - \left| \frac{Z_{in}(\omega) - Z_0}{Z_{in}(\omega) + Z_0} \right|^2 \quad (1)$$

Where $Z_0 = 370\ \Omega$ and:

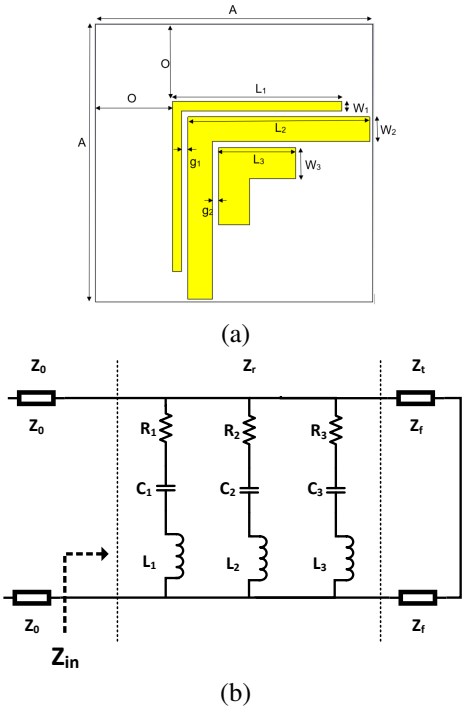

Fig. 1. Proposed structure, (a) Unit cell design, (b) Equivalent circuit

$$\frac{1}{Z_r(\omega)} = \frac{1}{R_1 + j\omega L_1 + \frac{1}{j\omega C_1}} + \frac{1}{R_2 + j\omega L_2 + \frac{1}{j\omega C_2}} + \frac{1}{R_3 + j\omega L_3 + \frac{1}{j\omega C_3}} \quad (2)$$

$$Z_t(\omega) = jZ_f tan(\beta l) = j\sqrt{\frac{\mu_r \mu_0}{\varepsilon_r \varepsilon_0}} tan(\frac{2\pi}{\lambda} h) \quad (3)$$

$$Z_{in}(\omega) = Z_r(\omega) + Z_t(\omega) \quad (4)$$

In above mentioned equations Z_f is the intrinsic impedance of FR-4 substrate, where ε_r and μ_r are relative permittivity and permeability, respectively.

Additional to the equivalent circuit and absorbing equations, parametric study has been done to optimize the final result and investigate the effect of different parameters on the absorbance. The length of resonators is an important factor of absorber due to specifying the absorption frequencies. Fig. 2 (a-c) shows the absorbance of proposed structure by changing L_1, L_2 and L_3 in ranges of 1190-1990 um, 1040-1840 um and 580-1380 um, respectively. Moreover, the resonators width affects the bandwidth of absorption due to the changing inductive and capacitive properties of the structure. The results of various values of W_1, W_2, and W_3 in ranges of 22.5-122.5 um, 190-310 um, and 220-420 um are shown in Fig. 2 (d-f). The gaps between resonators and the free space gap between the unit cell (g_1 and g_2) and the left and top neighbors (O) are two other parameters that have been investigated and the results are illustrated in Fig. 2 (g-i). The final dimensions of the structure

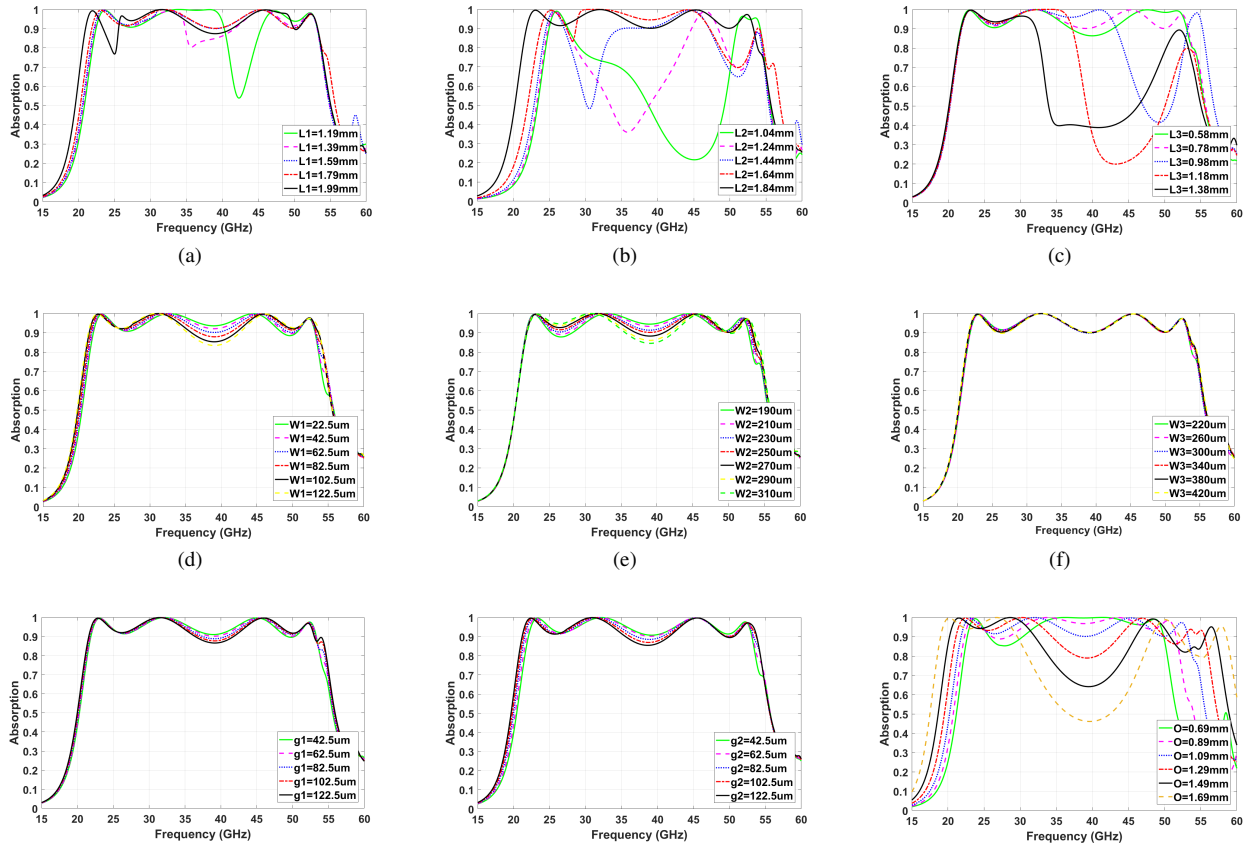

Fig. 2. The absorption characteristic by changing, (a) First resonator length (L_1), (b) Second resonator length (L_2), (c) Third resonator length (L_3), (d) First resonator width (W_1), (e) Second resonator width (W_2), (f) Third resonator width (W_3), (g) Upper gap (g_1), (h) Lower gap (g_2)), (i) Offset of resonators (O)

TABLE I
FINAL VALUES OF PARAMETERS

Par	A	L_1	L_2	L_3	W_1	W_1	W_3	g_1	g_2	O
Value (um)	2810	1790	1840	780	62.5	250	300	62.5	62.5	1090

are shown in Table I that guarantees more than 90% absorption ratio for the frequency range of 21.79 GHz to 53.23 GHz.

The relative absorption band (RAB) or fractional bandwidth is an index to compare bandwidth of microwave structure which is defined as:

$$RAB = 2 \times \frac{f_U - f_L}{f_U + f_L} \tag{5}$$

Where f_U and f_L are the upper and lower frequencies with a specific absorption ratio, respectively. By considering 90% as the lowest absorption ratio, the RAB factor of the final structure is 83.81%, where $f_L = 21.79$ GHz and $f_U = 53.23$ GHz. To highlight the performance, the designed MPA in this paper has been compared with the recently reported ultra wideband structure in Table II.

TABLE II
CHARACTERISTICS COMPARISON

Ref	f_L (GHz)	f_U (GHz)	RAB (%)	Number of Layers	Lumped element
[12]	12.80	16.64	26	1	No
[13]	9.4	11.7	21.8	1	No
[17]	10	22	58.8	2	Yes
[19]	10	21	58	4	Yes
[25]	4	8	66.67	1	No
Proposed structure	21.8	53.2	83.81	1	No

III. RESULTS AND DISCUSSION

To explain how the structure works, the electric field are accomplished at four frequencies with higher absorption ratios which are $f = 23.16$ GHz, $f = 32.04$ GHz, $f = 45.16$ GHz, and $f = 52.53$ GHz. As it is shown in Fig. 3 (a-d) the concentration of the electric field is mainly in the edges of the structure. At $f = 23.16$ GHz, the outer parts of the resonators mainly are responsible for trapping signals. However, by increasing the frequency, the engagement of inner resonator increases, and at $f = 52.53$ GHz, the electric

field focus point is on the edge of the smallest part. Adding two L-shape metal paths to the main resonator increases the capacitive characteristic of metamaterial absorber which leads to shifting lower frequency downward, and increasing the trapped signal in the gap between them.

Having stable absorptivity facing different incident angles is a crucial point for MPAs. Fig. 4 (a) and (b) show the absorption variation when the incident wave angle is increased from 0 to 70 degree for TE and TM modes, respectively. The absorptivity of the proposed structure remains higher than 75% for incident angle up to 40 degree in the majority of absorption bandwidth. For higher incident angles, the bandwidth starts decreasing. However, the range of 0-40 degree covers a large number of incident signals with both TE and TM polarization.

The situation is upside down for different polarization angles. The proposed structure works as a polarization angle selective metamaterial surface. The L-shape resonator leads to a dual-polarization structure which absorbs for horizontal and vertical polarization wave perfectly. On the other hand, as Fig.4 (c) and (d) show, the absorption ratio decreases significantly for higher polarization angles. The absorption of structure drops around 15% and 30% for $\phi = 10$ and 80 and $\phi = 20$ and 70, respectively.

IV. Conclusion

In this paper, an ultra-wideband metamaterial absorber has been designed on FR-4 as a substrate, which leads to low-profile structure. Instead of using lumped element, three L-shape resonators have been etched on top of the structure with close resonance frequencies. The absorption bandwidth of the proposed structure is more than 20 GHz, which covers most of the 5G spectrum. The size of the unit cell is $2.81mm \times 2.81mm \times 1mm$ which is $0.2\lambda \times 0.2\lambda$ at the lowest frequency with more than 90% absorption efficiency. The design is verified by full-wave simulation. The results show that the structure works for both horizontal and vertical polarization and shows a reasonable insensitivity facing different incident angles.

References

[1] M. Amiri, F. Tofigh, N. Shariati, J. Lipman, and M. Abolhasan, "Miniature tri-wide band sierpinski-minkowski fractals metamaterial perfect absorber," *IET Microwaves, Antennas & Propagation*, 2019.

[2] F. Costa, S. Genovesi, A. Monorchio, and G. Manara, "Low-cost metamaterial absorbers for sub-ghz wireless systems," *IEEE Antennas and Wireless Propagation Letters*, vol. 13, pp. 27–30, 2014.

[3] Y. Peng, X. Zang, Y. Zhu, C. Shi, L. Chen, B. Cai, and S. Zhuang, "Ultra-broadband terahertz perfect absorber by exciting multi-order diffractions in a double-layered grating structure," *Optics express*, vol. 23, no. 3, pp. 2032–2039, 2015.

[4] D. Hu, H.-y. Wang, and Q.-f. Zhu, "Design of six-band terahertz perfect absorber using a simple u-shaped closed-ring resonator," *IEEE Photonics Journal*, vol. 8, no. 2, pp. 1–8, 2016.

[5] J. Hao, L. Zhou, and M. Qiu, "Nearly total absorption of light and heat generation by plasmonic metamaterials," *Physical review B*, vol. 83, no. 16, p. 165107, 2011.

[6] M. Diem, T. Koschny, and C. M. Soukoulis, "Wide-angle perfect absorber/thermal emitter in the terahertz regime," *Physical Review B*, vol. 79, no. 3, p. 033101, 2009.

[7] M. Hajizadegan, V. Ahmadi, and M. Sakhdari, "Design and analysis of ultrafast and tunable all optical metamaterial switch enhanced by metal nanocomposite," *Journal of Lightwave Technology*, vol. 31, no. 12, pp. 1877–1883, 2013.

[8] X. Liu, J. Zhou, N. Litchinitser, and J. Sun, "Metamaterial all-optical switching based on resonance mode coupling in dielectric meta-atoms," *arXiv preprint arXiv:1412.3338*, 2014.

[9] B. Ghaderi, V. Nayyeri, M. Soleimani, and O. M. Ramahi, "Pixelated metasurface for dual-band and multi-polarization electromagnetic energy harvesting," *Scientific reports*, vol. 8, no. 1, p. 13227, 2018.

[10] H.-T. Zhong, X.-X. Yang, C. Tan, and K. Yu, "Triple-band polarization-insensitive and wide-angle metamaterial array for electromagnetic energy harvesting," *Applied Physics Letters*, vol. 109, no. 25, p. 253904, 2016.

[11] T. S. Almoneef, F. Erkmen, and O. M. Ramahi, "Harvesting the energy of multi-polarized electromagnetic waves," *Scientific reports*, vol. 7, no. 1, p. 14656, 2017.

[12] R. Sekar and S. R. Inabathini, "An ultra-thin compact wideband metamaterial absorber," *Radioengineering*, vol. 27, no. 2, p. 365, 2018.

[13] S. Ramya and I. S. Rao, "An ultra-thin, bandwidth enhanced metamaterial absorber for x-band applications," *Wireless Personal Communications*, vol. 105, no. 4, pp. 1617–1627, 2019.

[14] S. Li, J. Gao, X. Cao, W. Li, Z. Zhang, and D. Zhang, "Wideband, thin, and polarization-insensitive perfect absorber based the double octagonal rings metamaterials and lumped resistances," *Journal of Applied Physics*, vol. 116, no. 4, p. 043710, 2014.

[15] S. Ramya and I. Srinivasa Rao, "A compact ultra-thin ultra-wideband microwave metamaterial absorber," *Microwave and Optical Technology Letters*, vol. 59, no. 8, pp. 1837–1845, 2017.

[16] S. D. Assimonis and V. Fusco, "Polarization insensitive, wide-angle, ultra-wideband, flexible, resistively loaded, electromagnetic metamaterial absorber using conventional inkjet-printing technology," *Scientific reports*, vol. 9, no. 1, pp. 1–15, 2019.

[17] L. L. Cong, X. Y. Cao, T. Song, J. Gao, and J. X. Lan, "Angular-and polarization-insensitive ultrathin double-layered metamaterial absorber for ultra-wideband application," *Scientific reports*, vol. 8, no. 1, p. 9627, 2018.

[18] X. Begaud, A. Lepage, S. Varault, M. Soiron, and A. Barka, "Ultra-wideband and wide-angle microwave metamaterial absorber," *Materials*, vol. 11, no. 10, p. 2045, 2018.

[19] S.-J. Li, P.-X. Wu, H.-X. Xu, Y.-L. Zhou, X.-Y. Cao, J.-F. Han, C. Zhang, H.-H. Yang, and Z. Zhang, "Ultra-wideband and polarization-insensitive perfect absorber using multilayer metamaterials, lumped resistors, and strong coupling effects," *Nanoscale research letters*, vol. 13, no. 1, p. 386, 2018.

[20] J. Wei, Y. He, S. Bie, S. Wu, Z. Lei, W. Deng, Y. Liu, Y. Zhang, C. Li, J. Ai *et al.*, "Flexible design and realization of wideband microwave absorber with double-layered resistor loaded fss," *Journal of Physics D: Applied Physics*, vol. 52, no. 18, p. 185101, 2019.

[21] H.-F. Huang and B. Luo, "An ultra-wideband polarization independent metamaterial absorber based on on dual-polarization," in *2018 International Conference on Microwave and Millimeter Wave Technology (ICMMT)*. IEEE, 2018, pp. 1–3.

[22] W. Wang, H. Huang, B. Sima, B. Zhu, and Y. Feng, "A broadband metamaterial microwave absorber utilizing both magnetic and electric resonances," in *2018 Cross Strait Quad-Regional Radio Science and Wireless Technology Conference (CSQRWC)*. IEEE, 2018, pp. 1–3.

[23] H. Zhai, C. Zhan, L. Liu, and Y. Zang, "Reconfigurable wideband metamaterial absorber with wide angle and polarisation stability," *Electronics Letters*, vol. 51, no. 21, pp. 1624–1626, 2015.

[24] M. Aalizadeh, A. Khavasi, B. Butun, and E. Ozbay, "Large-area, cost-effective, ultra-broadband perfect absorber utilizing manganese in metal-insulator-metal structure," *Scientific reports*, vol. 8, no. 1, p. 9162, 2018.

[25] N. T. Q. Hoa, T. S. Tuan, L. T. Hieu, and B. L. Giang, "Facile design of an ultra-thin broadband metamaterial absorber for c-band applications," *Scientific reports*, vol. 9, no. 1, p. 468, 2019.

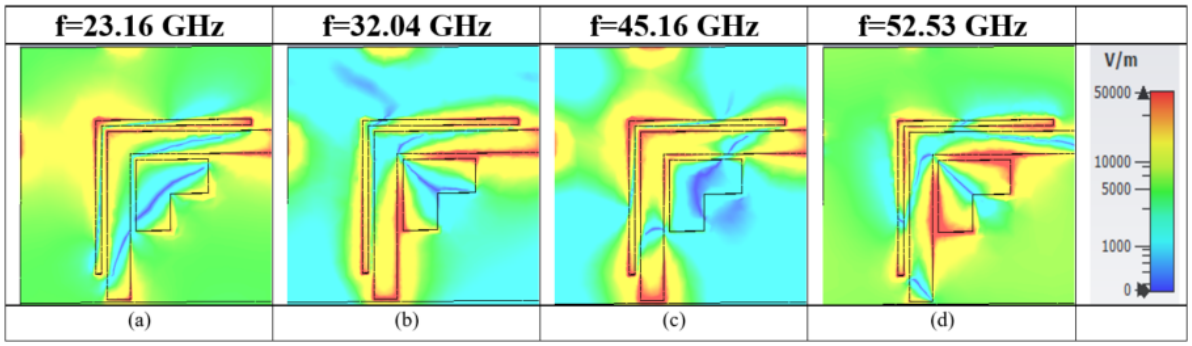

Fig. 3. Electirc field distribiurtion in (a) $f = 23.16GHz$, (b) $f = 32.04GHz$, (c) $f = 45.16GHz$, (d) $f = 52.53GHz$.

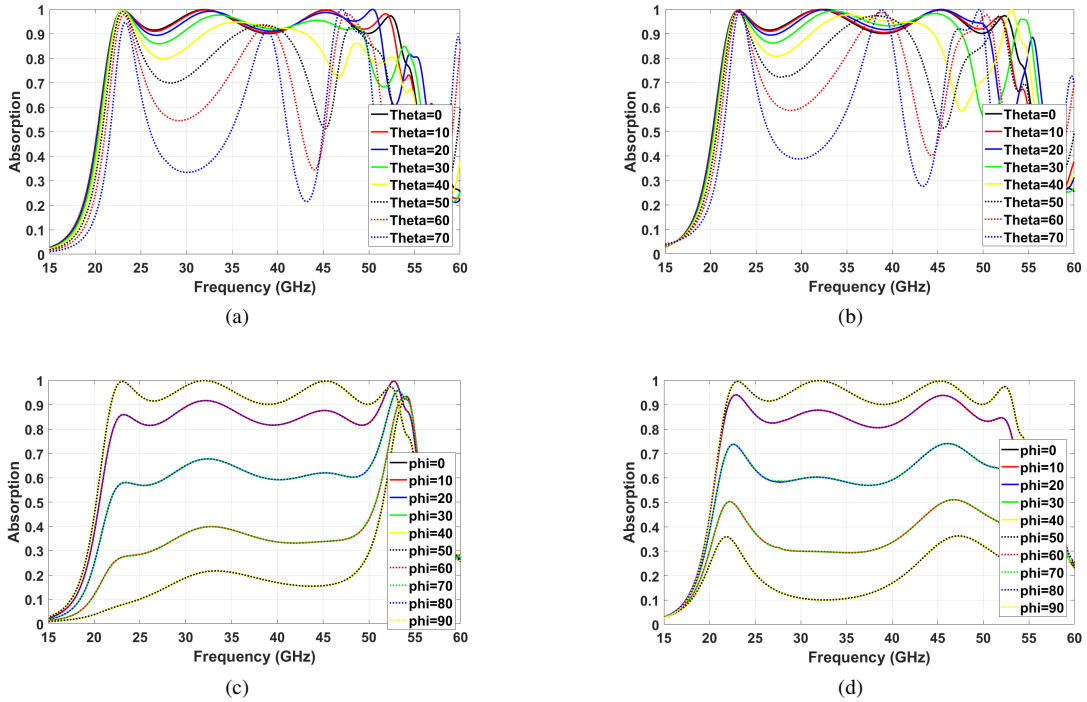

Fig. 4. Sensitivity of the proposed structure facing, (a) Different incident angles of TE mode waves, (b) Different incident angles of TM mode waves, (c) Different polarization angles of TE mode waves, (d) Different polarization angles of TM mode waves.